A Physical Human–Robot Interaction Framework for Trajectory Adaptation Based on Human Motion Prediction and Adaptive Impedance Control

Jing Luo, *Member, IEEE*, Chaoyi Zhang, Weiyong Si, Yiming Jiang, *Member, IEEE*, Chenguang Yang, *Fellow, IEEE*, and Chao Zeng, *Member, IEEE*

***Abstract*— Physical human-robot interaction (pHRI) plays an important role in robotic. In order for a human operator to be able to easily adapt to interact with a robot, a minimal interaction force in pHRI should be achieved. In this paper, a pHRI framework is proposed to allow the robot to regulate its trajectory adaptively for minimizing the interaction force with small position-tracking errors. The trajectory of the robot is first adjusted by the interaction force which is updated by the performance evaluation index. Then, the human hand motion is predicted based on the autoregressive (AR) model to further adapt the trajectory. Thirdly, an adaptive impedance control method is developed to update the stiffness in the robot impedance controller using surface electromyography (sEMG) signals for robot compliant interaction with the environment. This method allows the human operator to interact with the robot by the interaction force, the hand motion and muscle contraction. By investigating the performance of the proposed method, the interaction force is decreased and a good position tracking accuracy is achieved. Comparative experiments demonstrate the enhanced performance of the proposed method.**

Manuscript received 29 January 2024; revised 19 April 2024; accepted 10 June 2024. This article was recommended for publication by Associate Editor J. J. Liang and Editor Z. Li upon evaluation of the reviewers' comments. This work was supported in part by the National Natural Science Foundation (NSFC) under Grant 62203341, in part by the Natural Science Foundation of Hubei Province under Grant 2024AFB614, in part by the Natural Science Foundation of Chongqing under Grant CSTB2023NSCQ-MSX1078, in part by the UK Research and Innovation (UKRI) Postdoctoral Fellowships Guarantee under Grant EP/Z00117X/1, and in part by the State Key Laboratory of Robotics and Systems (HIT) under Grant SKLRS-2024-KF-09. *(Corresponding author: Chao Zeng.)*

Jing Luo is with the School of Automation, Wuhan University of Technology, Wuhan 430070, China, and also with Chongqing Research Institute, Wuhan University of Technology, Chongqing 430070, China (e-mail: jingluo@ieee.org).

Chaoyi Zhang is with the School of Automation, Wuhan University of Technology, Wuhan 430070, China (e-mail: chaoyizhang@whut.edu.cn).

Weiyong Si is with the School of Computer Science and Electronic Engineering, University of Essex, CO4 3SQ Essex, U.K. (e-mail: w.si@essex.ac.uk).

Yiming Jiang is with the School of Robotics and the National Engineering Research Center for Robot Visual Perception and Control Technology, Hunan University, Changsha 410012, China (e-mail: ymjiang@hnu.edu.cn).

Chenguang Yang and Chao Zeng are with the Department of Computer Science, University of Liverpool, L69 3BX Liverpool, U.K. (e-mail: cyang@ieee.org; chaozeng@ieee.org).

Color versions of one or more figures in this article are available at https://doi.org/10.1109/TASE.2024.3415650.

***Note to Practitioners*—This paper focuses on developing a novel method that can allow the robot to compliantly interact with the human operator while simultaneously taking into account the trajectory-tracking accuracy and the interaction force in pHRI scenarios. The proposed method has a large application potential in a variety of pHRI tasks, such as human-robot collaborative transporting, curing, assembly, cutting, and so on. In addition, the proposed method can allow the human operator to physically interact with the robot in an easier and more intuitive manner, by taking advantage of human motion prediction and adaptive impedance control. Therefore, it is also potentially utilized for rehabilitation and assistive robots, and robot learning skills from human physical demonstration.**

***Index Terms*— Physical human-robot interaction (pHRI), trajectory adaptation, adaptive impedance control, human motion prediction.**

I. Introduction

APPLICATIONS of robots have attracted more and more attention in recent years [1], [2], [3], [4], [5], [6]. However, in an increasing number of robotic applications, the physical interaction of a human with a robotic system is essential. Particularly for products that cannot be fully automated, the physical interaction between humans and robots is expected to improve the overall efficiency of various manufacturing tasks and processes. Physical human-robot interaction (pHRI) as a branch of robotics has penetrated every aspect of human society, such as in rehabilitation [7], industry [8] and agriculture [9]. It's also a hot topic, especially when the focus is on transporting, slicing, cutting, polishing tasks and so on [10] and [11]. When a human operator guides a robot to perform a tooling task, he or she must apply a certain force to the robot to move it along the planned trajectory and achieve a satisfactory performance. Performances largely depend on the the robot's ability of adapting their movements based on human intentions in pHRI tasks. Namely, the trajectory of the robot needs to be regulated to adapt to the human partner's motion.

Programming by demonstration (PbD) is usually used to allow the guidance of a robot's motion by a human operator [12], [13], [14]. The operator transmits trajectory information under specific tasks to the robot through

kinematics teaching and then the robot replicates the trajectory. However, PbD-based methods are not suitable when it comes to an uncertain environment. In [15], a robot controller was proposed to incorporate the estimated human's motion intention and make the robot proactively follow the human partner's movements. In [16], a method based on support vector machine and least squares method was proposed to improve robot execution ability. Reference [17] proposed an incremental motor skill learning, generalization and control method based on dynamic movement primitives (DMP) and broad learning system (BLS) for extracting skills from demonstrations. Reference [18] presented a skill learning-based control strategy by fusion with DMP and the Gaussian mixture model (GMM). Iterative learning control (ILC) is introduced to enhance the effectiveness of pHRI by trajectory regulation [19], [20], [21]. In [22], a spatial iterative learning control method is proposed for a robot to learn a desired path in an unknown environment. Since it's hard to precisely calculate intended motion trajectory, interaction control is applied in pHRI instead of pure motion control. In this case, the consideration of interaction force becomes necessary. The interaction force is used to instruct the robot's movement. In [23], a trajectory learning method based on iterative learning was proposed to improve tracking performance and the interaction force was used to regulate the trajectory. In [24], a spatial iterative learning algorithm which combines the interaction force and machine vision was proposed for online trajectory learning. Reference [25] proposed a new human-cooperative strategy to detect the human subject's motion intention extracted from the measurement of the subject's muscular effort. Reference [26] developed a trajectory adaptation method to guarantee the performance of collaboration tasks, the information of the interaction force was not only utilized to update the trajectory but also used to adjust the robot's impedance parameters. While the interaction force cannot effectively estimate human intentions. Enhanced performance in pHRI can be achieved if the robot can predict the human's trajectory and correspondingly adapt its own trajectory.

Human intention recognition is an important topic in the field of pHRI [27], [28]. It's necessary to utilize human intention to enhance the collaboration between human and the robot. In [29], a shared control method was proposed to recognize human intention. Reference [30] proposed to use Artificial Neural Network (ANN) to estimate the intentions of human. In [31], a haptic intention augmentation method was proposed to achieve safe interaction. Reference [32] proposed a human-in-the-loop control methodology for immersive training during the physical therapy, and the motion control of the robot in a compliant region is determined by humans. In [33], a novel method was proposed to recognize the implicit intention of a human user by using verbal communication, behavior recognition and motion recognition from the combination of machine learning, computer vision and voice recognition technologies. Moreover, human motion prediction can help recognize human intention. It can be easier for the robot to track the trajectory of the human by predicting his motion. In [34],a trajectory prediction method was proposed with the usage of contextual information for completing the corresponding tasks with the estimation confidence. In [35], a method of virtual reality based on K-means clustering and a hidden Markov model was proposed to predict human motion. Reference [36] proposed a Bayesian method to acquire the estimation of human stiffness obeying Gaussian distribution and human motion intention. In [37], a human motion prediction method based on autoregressive (AR) model was proposed for teleoperation and a virtual force model based on the haptic device was designed to correct the robot's trajectory. However, predicting human motion alone cannot meet the requirements of the pHRI tasks well. There are many other ways that can be combined with it to improve the performance.

It is popular to take advantages of biological signals which take an important part in pHRI. In [38], a simple recurrent neural network architecture was designed to predict human motion in a prediction window of 1 second to improve the performance in pHRI scenarios and achieve safer HRI. In [39], a novel approach was proposed to embed a human model in the robot's path planner and the costmap can be updated based on the observed or predicted states of the human. In [40], a novel Continual Learning (CL) approach was proposed for probabilistic human motion prediction which makes the robot continually learn during its interaction with collaborators. In fact, surface electromyography (sEMG) signals are widely used in these years [41]. The muscles activations which represent human stiffness can be obtained by sEMG signals and transferred to robots. Reference [42] proposed a method to estimate the stiffness of the human arm based on the agonist-antagonist muscular co-activations. Reference [43] developed a hybrid control that combines a brain-computer interface (BCI) based on motor imagery (MI) with sEMG signals to drive the exoskeleton and enhance human mobility. In [44], an sEMG-based control method was proposed to provide the robot with the information about the human behaviour and intention. In [45], a personalised variable gain control was developed and the control gain was obtained by sEMG signals so that the operator can interact with environment by muscle contraction. In addition, impedance/admittance control can work well for stiffness transfer. Reference [46] presented a pHRI interaction approach using admittance control to deal with a human subject's intention and online stiffness estimation to deal with the variable impedance property. Reference [47] developed a variable impedance control strategy to obtain information about the operator intentions based on EMG signals and include it into the robot control strategy. In [48], a novel adaptive impedance control algorithm was developed using sEMG signals to transfer stiffness from human operator. In [49], a pHRI system was proposed to map the estimated human arm stiffness extracted from EMG signals into the robot impedance controller.

According to above discussions, it's reasonable to apply both human intention recognition and interaction force in pHRI. sEMG signals can be also employed to further improve the performance in pHRI. Therefore, this paper develops a novel trajectory adaptation method based on both human

motion prediction and adaptive impedance control, in order to achieve compliant interactions. The information of the interaction force and human hand motion are both considered to regulate the trajectory of the robot. Besides, the stiffness of human arm is obtained and transferred to the robot for a better interaction. The interaction force can be decreased and the position tracking accuracy can be guaranteed. Our method allows the human user to complete the tasks to obtain a good performance in a comparatively easier manner without the need to predefine a fixed reference trajectory.

The contributions of this paper are as follows:

1) A novel pHRI strategy that integrates robot trajectory adaptation and human motion prediction is developed in this work, it allows the robot to physically interact with the operator with the consideration of human motion intention.
2) An improved adaptive impedance control method from [45] is introduced to the pHRI system to update the stiffness of the robot using sEMG signals, further decreasing the interaction force and enhancing the interaction between the human operator and the environment.
3) The proposed method is implemented on a Sawyer robot for pHRI tasks. Experimental results demonstrate the effectiveness of the proposed method. Compared with [26] and [37], the proposed method has a lower interaction force and a better interaction performance.

The rest of this article is structured as below. The problem preliminaries is described in Section II. The method including trajectory adaptation, human hand motion prediction and adaptive impedance control is described in Section III. Section IV analyses the results of experiments on a Sawyer robot. Section V is the discussions. Section VI concludes this work and lists future work.

II. Problem Preliminaries

In this work, a typical pHRI scenario is considered where a human operator cooperates with a robot to manipulate an object and there is no relative motion between the human hand, the object, and the robot. In the scenario, the robot regulates its trajectory by the interaction force imposed by the human operator.

The system dynamics of an n-degree-of-freedom (n-DOF) robot interacting with a human's upper limb in the joint space are described as:

$$M(q(t))\ddot{q}(t) + C(q(t), \dot{q}(t))\dot{q}(t) + G(q(t)) + D(\dot{q}(t)) = \tau(t) + J^T(t)F_h(t) \quad (1)$$

where $q(t) \in \mathbb{R}^n$ represents the joint angle. $\tau \in \mathbb{R}^n$ is control input vector of the robot and $F_h(t) \in \mathbb{R}^n$ represents the interaction force applied by the human operator. $M(q(t)) \in \mathbb{R}^{n\times n}$ is the inertia matrix, $C(q(t), \dot{q}(t)) \in \mathbb{R}^n$ is the Coriolis and centrifugal force, $G(q(t)) \in \mathbb{R}^n$ represents the gravitational force vector, and $D(\dot{q}(t)) \in \mathbb{R}^n$ denotes the friction matrix. $J(t) \in \mathbb{R}^{n\times n}$ is the Jacobian matrix.

For convenient analysis, the robot's dynamics are described in the Cartesian space when the physical interaction occurs at the robot's end-effector. So the system dynamics in the Cartesian space are given by:

$$M_x(t)\ddot{X}(t) + C_x(t)\dot{X}(t) + G_x(t) = J^{-T}(t)\tau(t) + F_h(t) \quad (2)$$

where $X(t)$ represents the trajectory of the robot's end-effector in the Cartesian space, and $\dot{X}(t)$, $M_x(t)$, $C_x(t)$, $G_x(t)$ are described as:

$$\dot{X}(t) = J(t)\dot{q}(t) \quad (3)$$

$$M_x(t) = J^{-T}(t)M(q(t))J^{-1}(t) \quad (4)$$

$$C_x(t) = J^{-T}(t)[C(q(t), \dot{q}(t)) - M(q(t))J^{-1}(t)\dot{J}(t)]J^{-1}(t) \quad (5)$$

$$G_x(t) = J^{-T}(t)(G(q(t)) + D(\dot{q}(t))) \quad (6)$$

According to human motor control [50], the interaction force is modeled as:

$$F_h(t) = -K(t)(X(t) - X_h(t)) \quad (7)$$

where $K(t) \in \mathbb{R}^{n\times n}$ is the stiffness matrix of the human's upper limb and $X_h(t) \in \mathbb{R}^n$ represents the expected trajectory. As a matter of fact, $F_h(t)$ can be measured by a force sensor.

Reducing the interaction force is key to pHRI. A minimal interaction force can not only reduce the workload but also improve efficiency. The following method is therefore developed to perform pHRI tasks with a minimal interaction force and a good position tracking accuracy.

III. Proposed Method

In this article, we propose a method to regulate the robot's trajectory by introducing trajectory adaptation into the human hand motion prediction. During the regulation, we also develop a method to update the impedance parameters of the robot. The structure of the proposed method is shown in Fig. 1. It can be seen that the prediction position and the interaction force determine the actual trajectory of the robot. In addition, the human operator is able to update the impedance parameters of the robot according to human muscle contractions. The details of trajectory adaptation, human hand prediction model and adaptive impedance control will be presented as below.

A. Trajectory Adaptation

The robot trajectory is adapted based on the interaction force and the current states, namely:

$$x_d(t) = \Psi(f_h(t), x(t)) \quad (8)$$

where $x_d(t) \in \mathbb{R}$ represents the updated reference trajectory of the robot, $x(t) \in \mathbb{R}$ represents the robot's current trajectory, $f_h(t) \in \mathbb{R}$ represents the interaction force on the end of the robot, Ψ is the function describing the relationship of $x(t)$, $x_d(t)$ and $f_h(t)$.

The interaction force can be used to update the robot's trajectory [26]. The updating law is as follows:

$$x_d(t) = \beta_1 f_h(t) + x(t) \quad (9)$$

where $\beta_1 = B_1\alpha_1$ is a parameter to adjust the interaction force, B_1 is used to adjust β_1 and α_1 need to be constantly updated.

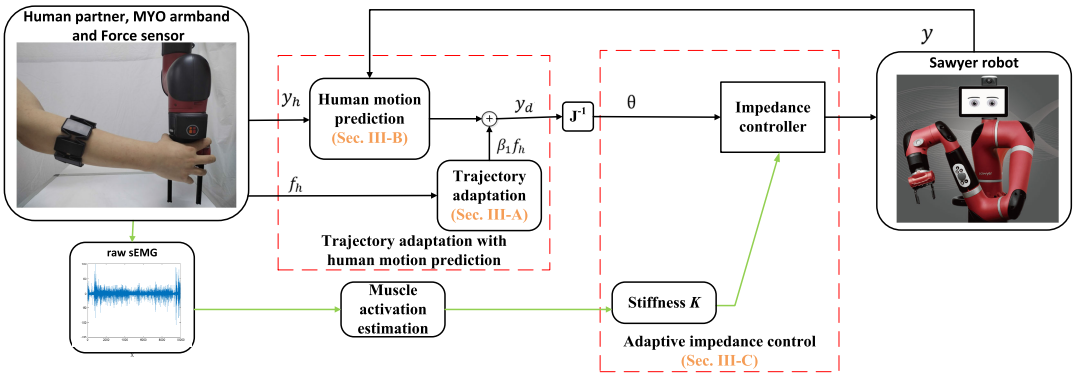

Fig. 1. The structure of the proposed method.

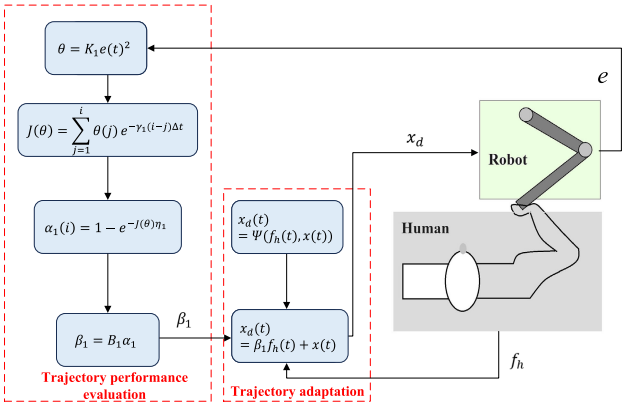

Fig. 2. The scheme of trajectory adaptation.

The expected trajectory and the actual trajectory determine the deviation ($e(t) = x(t) - x_d(t)$). The relationship of position error and the interaction force is written as follows [51]:

$$\theta = K_1 e(t)^2 \tag{10}$$

where θ represents a performance evaluation index and K_1 represents a parameter to adjust the deviation $e(t)$. The function $J(\theta)$ which is used to regulate α_1 can be defined as follows:

$$J(\theta) = \sum_{j=1}^{i} \theta(j) e^{-\gamma_1 (i-j)\Delta t} \tag{11}$$

where i is the sampling number, Δt is the sampling time, γ_1 is aim to adjust the forgetting rate. With the above definitions, α_1 is calculated by:

$$\alpha_1(i) = 1 - e^{-J(\theta)\eta_1} \tag{12}$$

where e is the natural index and η_1 is a parameter to regulate the interaction force.

By using trajectory adaptation, the robot can adjust the trajectory by the interaction force and follow human motion actively. The structure of trajectory adaptation is shown in Fig. 2.

B. Human Motion Prediction

Autoregression model (AR model) is a time series model that uses observations from previous time steps as input to a regression equation to predict the value at the next time step. In this article AR model is employed to predict the human hand motion which can be described as a time series model. The definition of p-order AR model is as follows [37]:

$$x_t = \phi_0 + \phi_1 x_{t-1} + \phi_2 x_{t-2} + \cdots + \phi_p x_{t-p} + \epsilon_t \tag{13}$$

where x_t, x_{t-1}, $\cdots$, x_{t-p} represent time series data, ϕ_0, $\phi_1, \cdots, \phi_p$ represent autoregression parameters which need to be determined, ϵ_t represents the white noise. The AR model can be described as a form of state space:

$$Q_t = U_t H_t + V_t \tag{14}$$

where $U_t = (x_{t-1}, x_{t-2}, \cdots, x_{t-p})$, $H_t = (\phi_0, \phi_1, \cdots, \phi_t)$ and $V_t = 0$. The human hand motion is assumed as a continuous trajectory as follows:

$$\begin{aligned} \dot{y}_h(t) = a_0 &+ a_1 y(t) + a_2 y(t-T) \\ &+ \cdots + a_i y(t-(i-1)T) \\ &+ \cdots + a_p y(t-(p-1)T) \end{aligned} \tag{15}$$

where $y(t) \in \mathbb{R}$ represents the actual trajectory of the human hand, $i = 0, 1, 2, \cdots, p$ represent the parameters that is determined by the type of human hand motion, T represents a time step. And Eq. (15) can be written as follows:

$$\dot{y}_h(t) = A^T W(t) \tag{16}$$

where $A^T = [a_0, a_1, a_2, \cdots, a_p]$, $W(t) = [1, y(t), y(t-T), \cdots, y(t-(p-1)T)]$. We can make the following approximation in order to obtain the value of $\dot{y}_h(t)$:

$$\dot{\hat{y}}_h = \hat{A}^T W(t) - \mu_1 \tilde{y}_h(t-T) \tag{17}$$

where $\tilde{y}_h(t-T) = \hat{y}_h(t-T) - y_h(t-T)$ is a deviation, $\hat{A}$ is the estimated value of A, μ_1 is a positive scalar.

In order to obtain the intention of human motion more accurately and correct the robot's trajectory, we introduce trajectory adaptation into the human hand prediction model. By employing trajectory adaptation, the desired trajectory of the robot is regulated by both the human hand motion and the interaction force. The interaction force is further adjusted by the method shown in Sec III. A. The updated law is as follows:

$$\dot{\hat{A}} = -(\tilde{y}_h(t-T) + \beta_1 f_h) W(t) \tag{18}$$

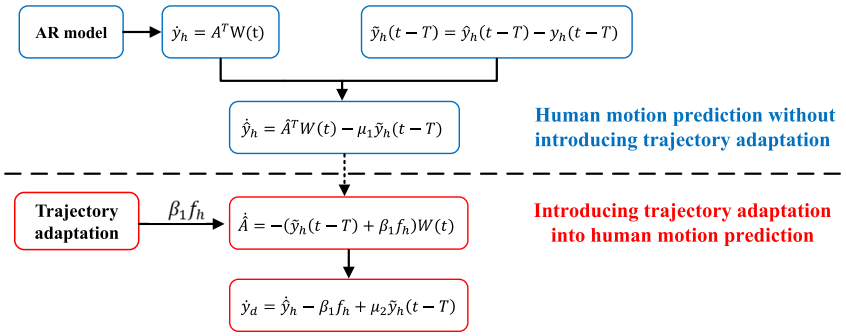

Fig. 3. The scheme of human motion prediction.

where β_1 and f_h have already been presented above. The desired trajectory of the robot is defined as follows:

$$\dot{y_d} = \dot{\hat{y}}_h - \beta_1 f_h + \mu_2 \tilde{y}_h(t-T) \tag{19}$$

where μ_2 is a positive scalar. The structure of human motion prediction is shown in Fig. 3.

C. Adaptive Impedance Control

We further explore adaptive impedance control to improve the interaction performance. The impedance control model is usually given as follows:

$$M_d \ddot{X}_e + D_d \dot{X}_e + K_d X_e = F_{ext} \tag{20}$$

where $M_d \in \mathbb{R}^{3\times3}$, $D_d \in \mathbb{R}^{3\times3}$, and $K_d \in \mathbb{R}^{3\times3}$ represent the expected inertia, damping and stiffness parameters, $F_{ext} \in \mathbb{R}^3$ represents the external force. In this article, the adaptation of the stiffness K_d is achieved using the sEMG signals, namely, the variable stiffness profile is transferred from human operator to the robot and position error $X_e \in \mathbb{R}^3$ is not considered.

A processing procedure is needed to obtain the sEMG-based stiffness, as shown in Fig. 4. The raw sEMG signals from all channels are processed as follows:

$$s_0(t) = \sum_{i=1}^{N} \sqrt{s_i^2(t)} \tag{21}$$

where N represents the number of channels and $s_i(t) \in \mathbb{R}$ represents the raw sEMG signal. After low-pass filter and normalization, $s_0(t)$ becomes $s(t)$. The neural activation model is as follows:

$$u(t) = B_1 s(t-d) + B_2 u(t-1) + B_3 u(t-2) \tag{22}$$

where B_1, B_2, B_3 are parameters which need to be determined and d is delay time. The nonlinear mapping from neural activation to muscle activation is realized as follows:

$$a(t) = \frac{e^{Cu(t)-1}}{e^C - 1} \tag{23}$$

where e is the natural index and C is the nonlinear shape factor. The variable stiffness is defined as follows [45]:

$$K(t) = (K_{max} - K_{min}) \frac{a(t) - a_{min}}{a_{max} - a_{min}} + K_{min} \tag{24}$$

where $K(t)$ is the stiffness of the human's upper limb. It's noted that K_{max}, K_{min}, a_{max}, a_{min} are obtained experimentally beforehand. By the proposed adaptive impedance control, the human operator can adjust the stiffness of the robot so that they can interact with the environment better.

With trajectory adaptation, human hand motion prediction and adaptive impedance control, the robot's trajectory can be regulated accurately and the interaction force can be decreased.

IV. Experiments

In the section, we validate the efficiency of the proposed method by designing comparative experiments.

A. Experimental Setup

Experiments are performed on a Sawyer robot which is a 7-DOF robot arm and the human operator can complete pHRI tasks with it. The sEMG signals are obtained by a MYO armband. MYO has a default sampling frequency of 200Hz and 8 channels. It can be wore by the human operator easily. Robot operation system (ROS) is used to integrate the system through the ROS topics. The experimental platform is shown in Fig. 5.

In the experiments, different tasks are performed with three different methods.

- Condition 1: Trajectory adaptation (TA). The robot's trajectory is only regulated by the interaction force.
- Condition 2: Trajectory adaptation with human motion prediction (TA-HMP). The human motion is predicted to be an adjustment to the robot's trajectory, and the interaction force is used to further adapt the trajectory.
- Condition 3: Trajectory adaptation with human motion prediction and adaptive impedance control (TA-HMP&AIC). With trajectory adaptation and human motion prediction, the human operator can adjust the stiffness of the robot by introducing the proposed adaptive impedance control.

It's expected that the robot can follow human motion actively and the interaction can be achieved naturally between the human operator and the robot. The robot is unaware of the reference trajectory in advance. Therefore, the expected trajectory was drawn onto the whiteboard before the experiment for the human operator to follow. The aim of the experiments is to decrease the interaction force with a good position tracking accuracy. With a smaller interaction force, the human operator can more easily manipulate the robot to move to the desired place. From this point of view, the following position errors are used to demonstrate the effectiveness of the proposed method.

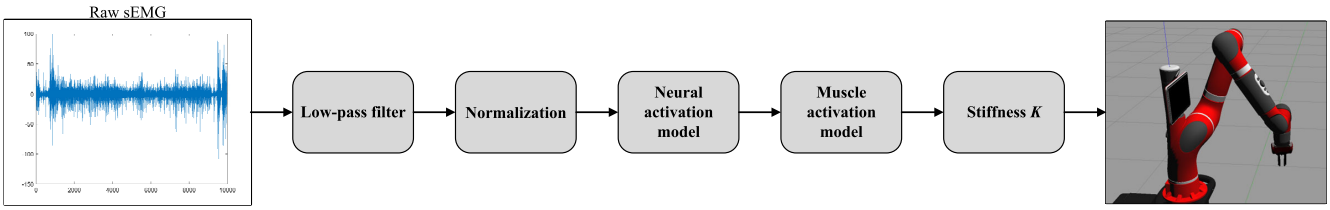

Fig. 4. The sEMG processing procedure for stiffness estimation.

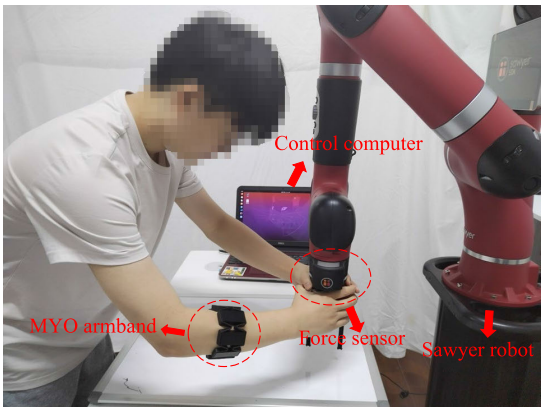

Fig. 5. The experimental platform.

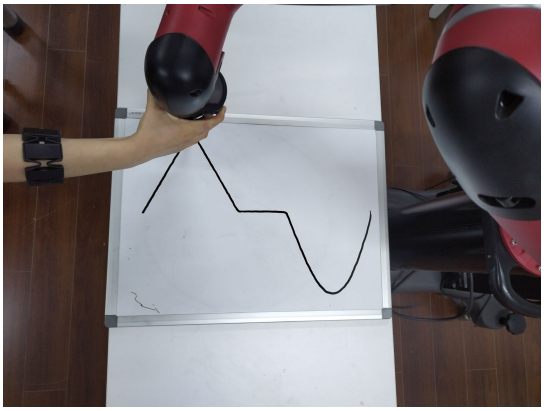

Fig. 6. The scene of Experiment 1.

The key parameters in the experiments are set as follows: K_1=10, γ_1=0.05, η_1=0.05, μ_1=5, μ_2=0.05. It's noted that a_{min}, a_{max}, K_{min}, and K_{max} need to be set according to different experimental subjects.

The position and the interaction force of the end-effector of the robot are recorded for subsequent analysis. The average absolute value of resultant force and the position error are employed to observe the performance of the proposed method. The following equation is used to treat the force in the X-axis (F_x) and Y-axis (F_y) as the resultant force (F).

$$F = \sqrt{F_x^2 + F_y^2} \tag{25}$$

Root-mean-square error (RMSE), mean absolute error (MAE) and roundness error (RE) are used to evaluate the position tracking accuracy.

$$RMSE = \sqrt{\frac{1}{m}\sum_{i=1}^{m}(y_1^{(i)} - y^{(i)})^2} \tag{26}$$

$$MAE = \frac{1}{m}\sum_{i=1}^{m}|y_1^{(i)} - y^{(i)}| \tag{27}$$

$$RE = \frac{1}{m}\sum_{i=1}^{m}|\sqrt{(x_1^{(i)} - x_0)^2 + (y_1^{(i)} - y_0)^2} - r| \tag{28}$$

where m is the number of data, i is the sampling number, y is the true value and x_1, y_1 denote the measured value. x_0, y_0 denote the centre of the circle and r is the radius. The proposed RE method allows the accuracy of the circle to be estimated from the distance between the resulting trajectory and the centre of the circle, and is easy to implement.

B. Experiment 1

In Experiment 1, three different methods are used to perform a pHRI task. The human operator cooperates with the sawyer robot while following an expected trajectory. To simplify the experiment, we regard the object as a point mass so that the trajectory of human hand is equivalent to the trajectory of the robot's end-effector. The scene of Experiment 1 is shown in Fig. 6. In order to emulate the complex process of transportation better, the expected trajectory is divided into different parts. The expected trajectory is as follows:

$$y = \begin{cases} 0.18\sin(5\pi(x-0.3)) & x \in [0.3, 0.5) \\ 0 & x \in [0.5, 0.6) \\ -1.8(x-0.6) & x \in [0.6, 0.7) \\ 1.8(x-0.8) & x \in [0.7, 0.8] \end{cases} \tag{29}$$

Fig. 7(a) shows the trajectory when performing experiments with TA, TA-HMP and TA-HMP&AIC. Fig. 7(b) shows the tracking performances and tracking errors. It can be seen that all of above methods can reach a good position accuracy. When it comes to a complex trajectory, the error variation is relatively large. Since it's hard for the human operator to follow accurately. The results of MAE and RMSE are presented in Fig. 9(a). It's shown that the proposed method can complete the task with a better position accuracy. It's easier to guide the robot follow the expected trajectory with human motion prediction and adaptive impedance control.

Parts of the interaction forces with TA, TA-HMP and TA-HMP&AIC are shown in Fig. 8(a). Since the robot may experience vibrations with TA, the interaction force in the X-axis and Y-axis sometimes fluctuates a lot. However, the

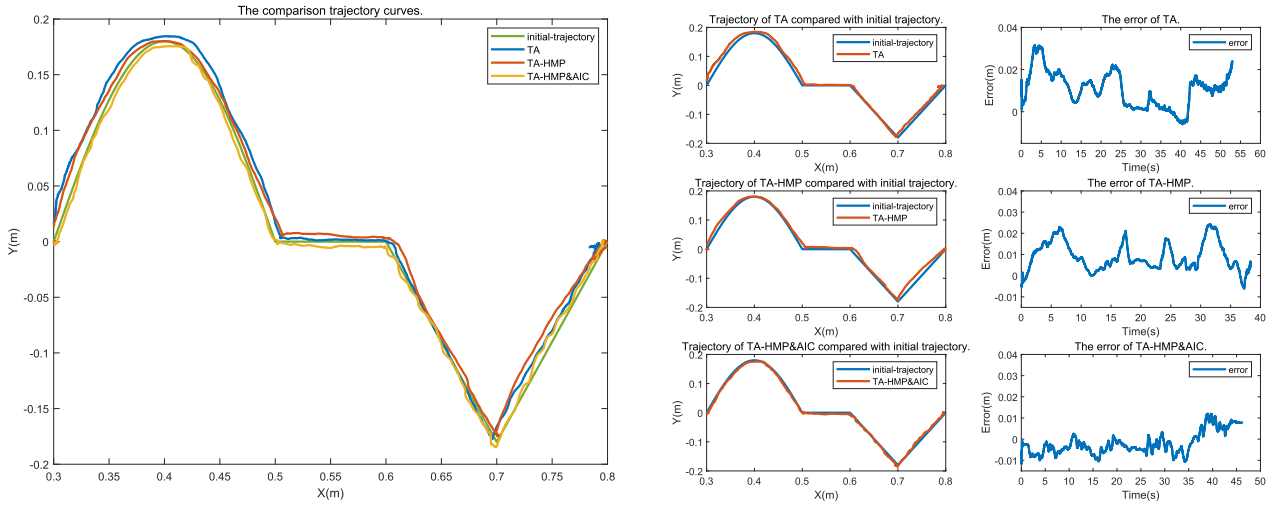

(a) The trajectory of the robot.

(b) Tracking performances and tracking errors.

Fig. 7. The trajectories with TA, TA-HMP and TA-HMP&AIC in Experiment 1.

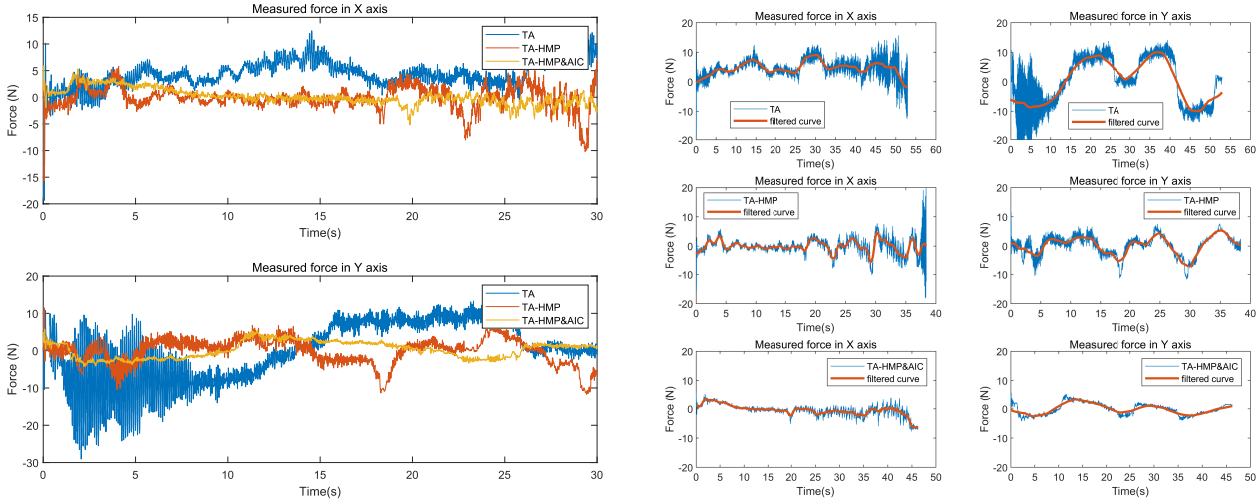

(a) The collected force profiles.

(b) The interaction force.

Fig. 8. The interaction forces with TA, TA-HMP and TA-HMP&AIC in Experiment 1.

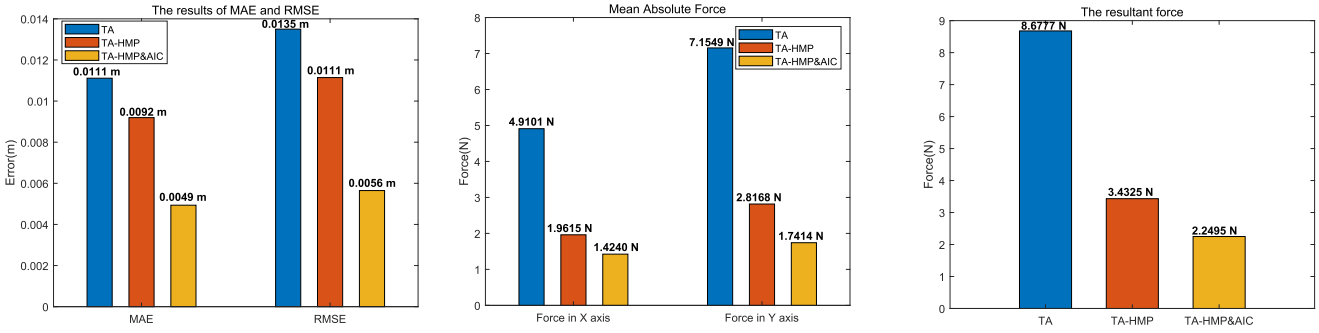

(a) The results of MAE and RMSE.

(b) The results of the mean force.

(c) The results of the resultant force.

Fig. 9. The results obtained by TA, TA-HMP and TA-HMP&AIC in Experiment 1.

interaction force is more stable with human motion prediction and adaptive impedance control. With the proposed method, the vibration becomes weaker. Fig. 8(b) shows the interaction force and the interaction force with the process of moving average filtering with TA, TA-HMP and TA-HMP&AIC, respectively. The filtered curves can better compare the

TABLE I
THE RESULTANT FORCE, MAE AND RMSE IN EXPERIMENT 1

	TA	TA-HMP	TA-HMP&AIC
MAE(M)	0.0111	0.0092	**0.0049**
RMSE(M)	0.0135	0.0111	**0.0056**
Resultant force(N)	8.6777	3.4325	**2.2495**

TABLE II
THE RESULTANT FORCE(N) IN EXPERIMENT 1

	Subject 1	Subject 2	Subject 3	Subject 4	Subject 5
TA	8.6777	7.1617	8.2307	8.1445	9.1093
TA-HMP	3.4325	3.5549	3.8611	3.1925	3.4616
TA-HMP&AIC	**2.2495**	**2.8665**	**3.0208**	**2.7052**	**2.7929**

Fig. 10. The scene of Experiment 2.

magnitude of the interaction force. Fig. 9(b) shows the mean absolute force in the X-axis and Y-axis and Fig. 9(c) shows the resultant force.

It can be seen that the proposed method can achieve a minimized interaction force in the pHRI task. By proposed method, the human operator can cooperate with the robot easily. The resultant force and the results of MAE and RMSE in Experiment 1 are presented in Table I. In order to further verify the interaction force among different methods, five subjects were selected for the experiment. Table II shows the resultant force by different methods in the five subjects' experiment. From this Table, it can be seen that the proposed method can obtain the best performance.

C. Experiment 2

In Experiment 2, the same methods as Experiment 1 are used to perform a different pHRI task. The human operator cooperates with the robot to transport a box. The trajectory of human hand is obtained by the trajectory of the robot's end-effector and the size of the box. The scene of Experiment 2 is shown in Fig. 10. The expected trajectory is as follows:

$$(x - 0.6)^2 + y^2 = 0.04 \tag{30}$$

Fig. 11 shows the tracking performances with these three methods, i.e., TA, TA-HMP and TA-HMP&AIC. The results of roundness error is shown in Fig. 13(a). Similar to the results in

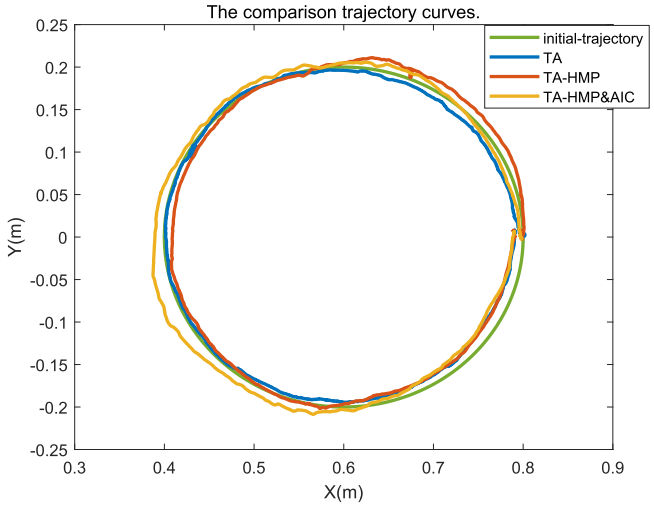

Fig. 11. The trajectories with TA, TA-HMP and TA-HMP&AIC in Experiment 2.

Experiment 1, the proposed TA-HMP&AIC method achieves the best position tracking accuracy.

Fig. 12 shows parts of the interaction force with TA, TA-HMP and TA-HMP&AIC. Fig. 13(b) shows the mean absolute force in the X-axis and Y-axis and Fig. 13(c) shows the resultant force. It is clear to see that the proposed method achieves a minimized interaction force and the weakest vibration. Although the interaction force in X-axis of TA-HMP&AIC is higher than that of TA-HMP, the resultant force of TA-HMP&AIC is still the smallest. The resultant force and the result of roundness error in Experiment 2 are also presented in Table III. Table IV shows the resultant force by different methods for five subjects. It can be seen that the proposed method has the minimum interaction force among the above mentioned methods.

The statistical results are presented in Fig. 14 and Table V-VII. It shows the interaction force results and the position error results by using TA, TA-HMP and TA-HMP&AIC. It can be seen that the proposed method obtains the smallest interaction force in the process of pHRI. With a smaller interaction force, the human operator can more easily manipulate the robot to move to the desired place, and the position accuracy can also be guaranteed. It's noted that the best position accuracy can be achieved in the appropriate high stiffness gain range.

In summary, the proposed method is tested by different experiments. The conclusion can be drawn that the proposed method can track the expected trajectory of human well while minimizing the interaction force. The human operator can complete pHRI tasks easier by the proposed method.

V. DISCUSSIONS

Comparative experiments in section IV demonstrate the performance of the proposed method, which achieves a minimized interaction force with a good position tracking accuracy. Trajectory adaptation is used to adjust the trajectory of the robot by the interaction force updated by the performance evaluation index. Compared to trajectory adaptation, the proposed method

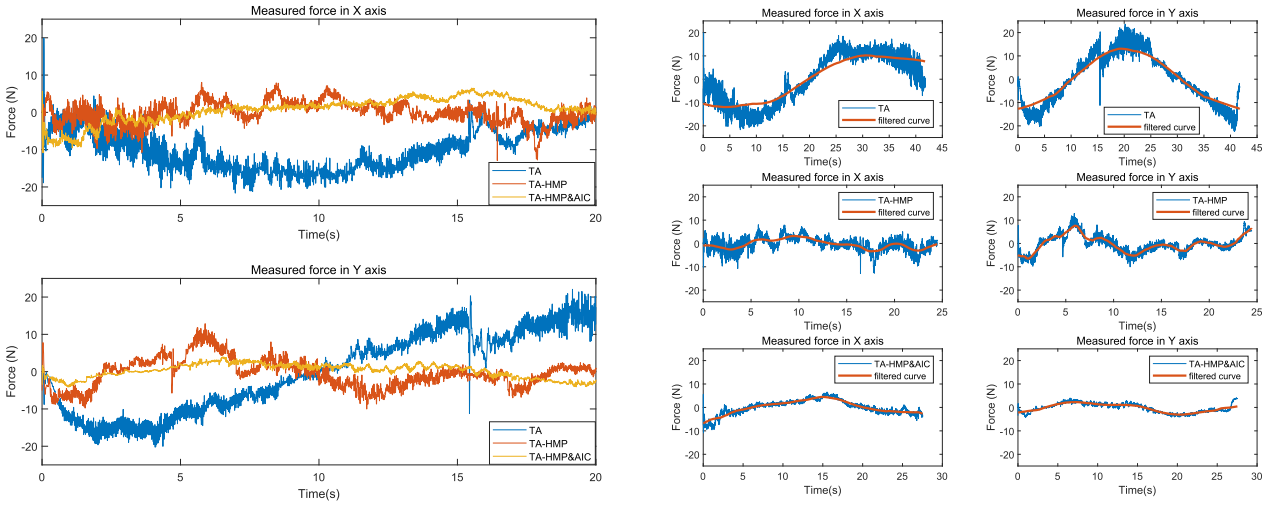

(a) The collected force profiles.

(b) The interaction force.

Fig. 12. The interaction forces with TA, TA-HMP and TA-HMP&AIC in Experiment 2.

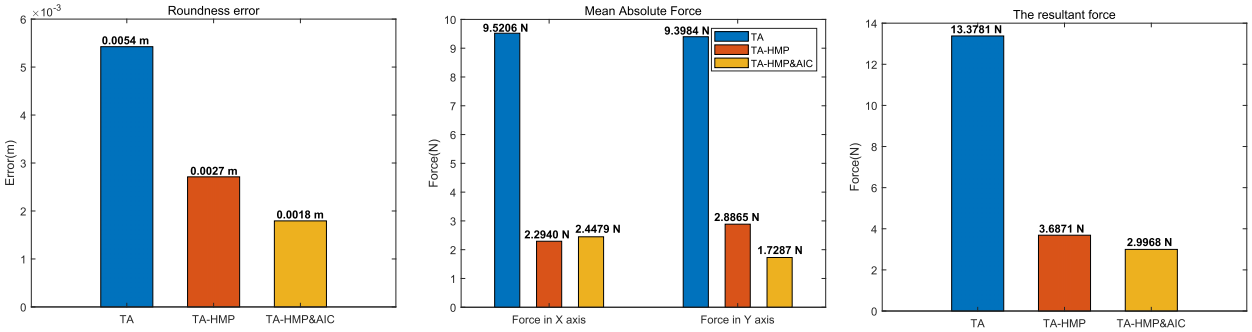

(a) The results of roundness error.

(b) The results of the mean force.

(c) The results of the resultant force.

Fig. 13. The results obtained by TA, TA-HMP and TA-HMP&AIC in Experiment 2.

can regulate the robot's trajectory by both the interaction force and prediction of human motion. By predicting human motion, the robot is aware of the intentions of human movements and the interaction force is effectively reduced. In contrast to trajectory adaptation with human motion prediction, adaptive impedance control is introduced to update the stiffness of the robot using sEMG signals. The interaction force is further reduced and the human operator can interact with the robot by muscle contraction for a better interaction.

Because of the physiological tremor of the human operator's hand, the interaction force of TA is significantly large and vibrates a lot. With the introduction of human motion prediction and adaptive impedance control, the effect of the human operator's physiological tremor is diminished and vibration becomes weaker. It also shows the adaptability of the proposed method to uncertain environments.

Additionally, five subjects take participate in the experiments to verify the robustness of the proposed method, and statistical experimental results show that the proposed TA-HMP&AIC can achieve the best performance among TA, TA-HMP and TA-HMP&AIC conditions.

The proposed method can be applied for various scenarios in pHRI. In fact, it shows great potential in path following tasks, i.e., welding, polishing and slicing. It can be also used for exoskeleton robots to transport objects with human users.

There are some limitations of the proposed method. If the human movement has significant uncertainties, the proposed method cannot be satisfying. Besides, the position error cannot be limited to a specific range because of the uncertainty of physical interaction. This may need introduce machine vision and advanced image extraction algorithms to improve the performances. In addition, three-dimensional cutting experiments

TABLE III

THE INTERACTION FORCE AND ROUNDNESS ERROR IN EXPERIMENT 2

	TA	TA-HMP	TA-HMP&AIC
Roundness error(M)	0.0054	0.0027	**0.0018**
Resultant force(N)	13.3781	3.6871	**2.9968**

TABLE IV

THE RESULTANT FORCE(N) IN EXPERIMENT 2

	Subject 1	Subject 2	Subject 3	Subject 4	Subject 5
TA	13.3781	10.8855	12.8196	13.2329	14.6521
TA-HMP	3.6871	3.5533	3.7282	3.9195	4.5337
TA-HMP&AIC	**2.9968**	**3.1530**	**2.9136**	**2.9394**	**2.6811**

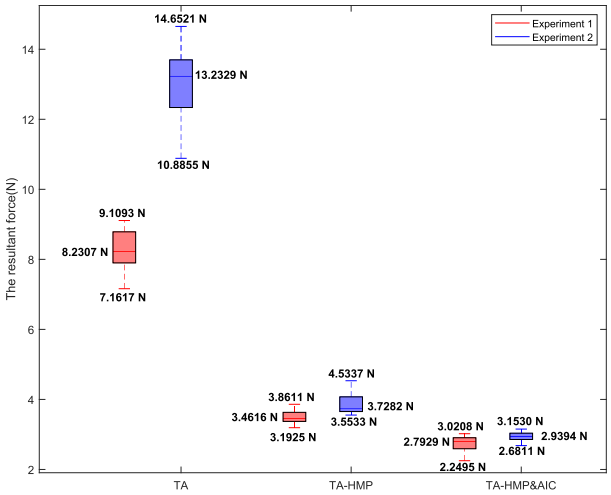

Fig. 14. Boxplot graphs of the resultant force using different methods in Experiment 1 and Experiment 2.

TABLE V
THE FORCE RESULTS OF DIFFERENT METHODS IN EXPERIMENT 1

Method	The resultant force(N)			
	Best force	Mean force	Worst force	Median force
TA	7.1617	8.2648	9.1093	8.2307
TA-HMP	3.1925	3.5005	3.8611	3.4616
TA-HMP&AIC	**2.2495**	**2.7270**	**3.0208**	**2.7929**

TABLE VI
THE FORCE RESULTS OF DIFFERENT METHODS IN EXPERIMENT 2

Method	The resultant force(N)			
	Best force	Mean force	Worst force	Median force
TA	10.8855	12.9936	14.6521	13.2329
TA-HMP	3.5533	3.8844	4.5337	3.7282
TA-HMP&AIC	**2.6811**	**2.9368**	**3.1530**	**2.9394**

TABLE VII
THE MEAN MAE, RMSE AND RE USING DIFFERENT METHODS FOR FIVE SUBJECTS IN EXPERIMENT 1 AND EXPERIMENT 2

	TA	TA-HMP	TA-HMP&AIC
MAE(M)	0.0107	0.0095	**0.0077**
RMSE(M)	0.0128	0.0118	**0.0091**
RE(M)	0.0071	0.0053	**0.0023**

will be designed to provide more focused results on the reduction of interaction force by the proposed method in future work.

VI. CONCLUSION

In this paper, a novel pHRI framework is proposed to allow the robot to regulate its trajectory adaptively. The human hand motion prediction based on AR model and the interaction force updated by the performance evaluation index are both considered to recognize the human intentions and regulate the robot's trajectory. In addition, sEMG signals is extracted for robot compliant interaction with the environment by transferring the human operator's stiffness to the robot. By the proposed method, the robot's trajectory can be regulated in a small position error and the interaction force can be decreased.

Experiments on a sawyer robot demonstrate the effectiveness of the proposed method. As shown by the experimental results, it's tough to reach a small interaction force with trajectory adaptation. While introducing trajectory adaptation into human motion prediction can further decrease the interaction force. Moreover, the interaction force can be minimized and the position accuracy can be guaranteed by the proposed method. The interaction between the human operator and the robot is improved. The robot can follow the human motion actively to reduce human burden and make the process of pHRI easier and more intuitive.

REFERENCES

[1] F. Romero and F. J. Alonso, "A comparison among different hill-type contraction dynamics formulations for muscle force estimation," *Mech. Sci.*, vol. 7, no. 1, pp. 19–29, Jan. 2016.

[2] P. Bujalski, J. Martins, and L. Stirling, "A Monte Carlo analysis of muscle force estimation sensitivity to muscle-tendon properties using a hill-based muscle model," *J. Biomechanics*, vol. 79, pp. 67–77, Oct. 2018.

[3] C. Dai, B. Bardizbanian, and E. A. Clancy, "Comparison of constant-posture force-varying EMG-force dynamic models about the elbow," *IEEE Trans. Neural Syst. Rehabil. Eng.*, vol. 25, no. 9, pp. 1529–1538, Sep. 2017.

[4] G. Hajian, A. Etemad, and E. Morin, "Automated channel selection in high-density sEMG for improved force estimation," *Sensors*, vol. 20, no. 17, p. 4858, Aug. 2020.

[5] J. Luo, Z. Lin, Y. Li, and C. Yang, "A teleoperation framework for mobile robots based on shared control," *IEEE Robot. Autom. Lett.*, vol. 5, no. 2, pp. 377–384, Apr. 2020.

[6] J. Luo, W. Liu, W. Qi, J. Hu, J. Chen, and C. Yang, "A vision-based virtual fixture with robot learning for teleoperation," *Robot. Auto. Syst.*, vol. 164, Jun. 2023, Art. no. 104414.

[7] R. V. Patel, S. F. Atashzar, and M. Tavakoli, "Haptic feedback and force-based teleoperation in surgical robotics," *Proc. IEEE*, vol. 110, no. 7, pp. 1012–1027, Jul. 2022.

[8] R. Jahanmahin, S. Masoud, J. Rickli, and A. Djuric, "Human–robot interactions in manufacturing: A survey of human behavior modeling," *Robot. Comput.-Integr. Manuf.*, vol. 78, Dec. 2022, Art. no. 102404.

[9] C. Véronneau et al., "Multifunctional remotely actuated 3-DOF supernumerary robotic arm based on magnetorheological clutches and hydrostatic transmission lines," *IEEE Robot. Autom. Lett.*, vol. 5, no. 2, pp. 2546–2553, Apr. 2020.

[10] X. Xing, K. Maqsood, D. Huang, C. Yang, and Y. Li, "Iterative learning-based robotic controller with prescribed human–robot interaction force," *IEEE Trans. Autom. Sci. Eng.*, vol. 19, no. 4, pp. 3395–3408, Oct. 2022.

[11] X. Xing, E. Burdet, W. Si, C. Yang, and Y. Li, "Impedance learning for human-guided robots in contact with unknown environments," *IEEE Trans. Robot.*, vol. 39, no. 5, pp. 3705–3721, Oct. 2023.

[12] G. Peng, C. L. P. Chen, and C. Yang, "Robust admittance control of optimized robot-environment interaction using reference adaptation," *IEEE Trans. Neural Netw. Learn. Syst.*, vol. 34, no. 9, pp. 5804–5815, Sep. 2023.

[13] G. Peng, C. Yang, Y. Li, and C. L. Philip Chen, "Impedance and trajectory adaptation for contact robots using integral reinforcement learning," in *Proc. 37th Youth Academic Annu. Conf. Chin. Assoc. Autom. (YAC)*, Nov. 2022, pp. 1542–1547.

[14] C. Yang, D. Huang, W. He, and L. Cheng, "Neural control of robot manipulators with trajectory tracking constraints and input saturation," *IEEE Trans. Neural Netw. Learn. Syst.*, vol. 32, no. 9, pp. 4231–4242, Sep. 2021.

[15] Y. Li, L. Yang, D. Huang, C. Yang, and J. Xia, "A proactive controller for human-driven robots based on force/motion observer mechanisms," *IEEE Trans. Syst., Man, Cybern., Syst.*, vol. 52, no. 10, pp. 6211–6221, Oct. 2022.

[16] C. Song, J. Xia, D. Huang, L. Ma, and Y. Li, "Path recognition and virtual guides design for path following based on human–robot collaboration," *IEEE Trans. Ind. Electron.*, vol. 70, no. 10, pp. 10374–10384, Oct. 2023.

[17] Z. Lu, N. Wang, M. Li, and C. Yang, "Incremental motor skill learning and generalization from human dynamic reactions based on dynamic movement primitives and fuzzy logic system," *IEEE Trans. Fuzzy Syst.*, vol. 30, no. 6, pp. 1506–1515, Jun. 2022.

[18] J. Li, Z. Li, X. Li, Y. Feng, Y. Hu, and B. Xu, "Skill learning strategy based on dynamic motion primitives for human–robot cooperative manipulation," *IEEE Trans. Cognit. Develop. Syst.*, vol. 13, no. 1, pp. 105–117, Mar. 2021.

[19] H. Huang, C. Yang, and C. L. P. Chen, "Optimal robot-environment interaction under broad fuzzy neural adaptive control," *IEEE Trans. Cybern.*, vol. 51, no. 7, pp. 3824–3835, Jul. 2021.

[20] Q. Li, W. Qi, Z. Li, H. Xia, Y. Kang, and L. Cheng, "Fuzzy-based optimization and control of a soft exosuit for compliant robot-human-environment interaction," *IEEE Trans. Fuzzy Syst.*, vol. 31, no. 1, pp. 241–253, Jan. 2023.

[21] C. Zeng, H. Su, Y. Li, J. Guo, and C. Yang, "An approach for robotic leaning inspired by biomimetic adaptive control," *IEEE Trans. Ind. Informat.*, vol. 18, no. 3, pp. 1479–1488, Mar. 2022.

[22] L. Yang, Y. Li, D. Huang, J. Xia, and X. Zhou, "Spatial iterative learning control for robotic path learning," *IEEE Trans. Cybern.*, vol. 52, no. 7, pp. 5789–5798, Jul. 2022.

[23] Y. Li and S. S. Ge, "Force tracking control for motion synchronization in human–robot collaboration," *Robotica*, vol. 34, no. 6, pp. 1260–1281, Jun. 2016.

[24] J. Xia, Y. Li, D. Huang, J. Yang, X. Xing, and L. Ma, "Spatial iterative learning control with human guidance and visual detection for path learning and tracking," *IEEE Trans. Autom. Sci. Eng.*, vol. 20, no. 3, pp. 1772–1784, Jul. 2023.

[25] Z. Li, B. Huang, A. Ajoudani, C. Yang, C.-Y. Su, and A. Bicchi, "Asymmetric bimanual control of dual-arm exoskeletons for human-cooperative manipulations," *IEEE Trans. Robot.*, vol. 34, no. 1, pp. 264–271, Feb. 2018.

[26] J. Luo, C. Yang, E. Burdet, and Y. Li, "Adaptive impedance control with trajectory adaptation for minimizing interaction force," in *Proc. 29th IEEE Int. Conf. Robot Human Interact. Commun. (RO-MAN)*, Aug. 2020, pp. 1360–1365.

[27] X. Yu, S. Liu, W. He, Y. Wu, H. Zhang, and Y. Wang, "A hybrid visual–haptic framework for motion synchronization in human–robot cotransporting: A human motion prediction method," *IEEE Robot. Autom. Mag.*, vol. 29, no. 4, pp. 25–35, Dec. 2022.

[28] X. Ren, Z. Li, M. Zhou, and Y. Hu, "Human intention-aware motion planning and adaptive fuzzy control for a collaborative robot with flexible joints," *IEEE Trans. Fuzzy Syst.*, vol. 31, no. 7, pp. 2375–2388, Jul. 2023.

[29] M. Gao, J. Oberländer, T. Schamm, and J. M. Zöllner, "Contextual task-aware shared autonomy for assistive mobile robot teleoperation," in *Proc. IEEE/RSJ Int. Conf. Intell. Robots Syst.*, Mar. 2014, pp. 3311–3318.

[30] K. Erdogan, A. Durdu, and N. Yilmaz, "Intention recognition using leap motion controller and artificial neural networks," in *Proc. Int. Conf. Control, Decis. Inf. Technol. (CoDIT)*, Apr. 2016, pp. 689–693.

[31] M. Panzirsch, R. Balachandran, J. Artigas, C. Riecke, M. Ferre, and A. Albu-Schaeffer, "Haptic intention augmentation for cooperative teleoperation," in *Proc. IEEE Int. Conf. Robot. Autom. (ICRA)*, May 2017, pp. 5335–5341.

[32] D. Wei et al., "Human-in-the-Loop control strategy of unilateral exoskeleton robots for gait rehabilitation," *IEEE Trans. Cognit. Develop. Syst.*, vol. 13, no. 1, pp. 57–66, Mar. 2021.

[33] M. W. C. N. Moladande and B. G. D. A. Madhusanka, "Implicit intention and activity recognition of a human using neural networks for a service robot eye," in *Proc. Int. Res. Conf. Smart Comput. Syst. Eng. (SCSE)*, Mar. 2019, pp. 38–43.

[34] M. Gao, R. Kohlhaas, and J. M. Zöllner, "Contextual learning and sharing autonomy to assist mobile robot by trajectory prediction," in *Proc. IEEE Int. Symp. Saf., Secur., Rescue Robot. (SSRR)*, Oct. 2016, pp. 274–275.

[35] Q. Wang, W. Jiao, R. Yu, M. T. Johnson, and Y. Zhang, "Modeling of human welders' operations in virtual reality human–robot interaction," *IEEE Robot. Autom. Lett.*, vol. 4, no. 3, pp. 2958–2964, Jul. 2019.

[36] X. Yu et al., "Bayesian estimation of human impedance and motion intention for human–robot collaboration," *IEEE Trans. Cybern.*, vol. 51, no. 4, pp. 1822–1834, Apr. 2021.

[37] J. Luo, D. Huang, Y. Li, and C. Yang, "Trajectory online adaption based on human motion prediction for teleoperation," *IEEE Trans. Autom. Sci. Eng.*, vol. 19, no. 4, pp. 3184–3191, Oct. 2022.

[38] M. El-Shamouty and A. Pratheepkumar, "PredNet: A simple human motion prediction network for human–robot interaction," in *Proc. 26th IEEE Int. Conf. Emerg. Technol. Factory Autom. (ETFA)*, Sep. 2021, pp. 1–7.

[39] M. Faroni, M. Beschi, and N. Pedrocchi, "Safety-aware time-optimal motion planning with uncertain human state estimation," *IEEE Robot. Autom. Lett.*, vol. 7, no. 4, pp. 12219–12226, Oct. 2022.

[40] J. Xu, S. Wang, X. Chen, J. Zhang, X. Lan, and N. Zheng, "A continuous learning approach for probabilistic human motion prediction," in *Proc. Int. Conf. Robot. Autom. (ICRA)*, May 2022, pp. 11222–11228.

[41] X. Chen, Y. Jiang, and C. Yang, "Stiffness estimation and intention detection for human–robot collaboration," in *Proc. 15th IEEE Conf. Ind. Electron. Appl. (ICIEA)*, Nov. 2020, pp. 1802–1807.

[42] A. Ajoudani, N. G. Tsagarakis, and A. Bicchi, "Tele-impedance: Towards transferring human impedance regulation skills to robots," in *Proc. IEEE Int. Conf. Robot. Autom.*, May 2012, pp. 382–388.

[43] Z. Li et al., "Hybrid brain/muscle signals powered wearable walking exoskeleton enhancing motor ability in climbing stairs activity," *IEEE Trans. Med. Robot. Bionics*, vol. 1, no. 4, pp. 218–227, Nov. 2019.

[44] L. Peternel, N. Tsagarakis, and A. Ajoudani, "A human–robot co-manipulation approach based on human sensorimotor information," *IEEE Trans. Neural Syst. Rehabil. Eng.*, vol. 25, no. 7, pp. 811–822, Jul. 2017.

[45] C. Yang, J. Chen, Z. Li, W. He, and C.-Y. Su, "Development of a physiological signals enhanced teleoperation strategy," in *Proc. IEEE Int. Conf. Inf. Automat.*, 2015, pp. 13–19.

[46] Z. Li, B. Huang, Z. Ye, M. Deng, and C. Yang, "Physical human–robot interaction of a robotic exoskeleton by admittance control," *IEEE Trans. Ind. Electron.*, vol. 65, no. 12, pp. 9614–9624, Dec. 2018.

[47] M. Bednarczyk, H. Omran, and B. Bayle, "EMG-based variable impedance control with passivity guarantees for collaborative robotics," *IEEE Robot. Autom. Lett.*, vol. 7, no. 2, pp. 4307–4312, Apr. 2022.

[48] Z. Li, Z. Huang, W. He, and C.-Y. Su, "Adaptive impedance control for an upper limb robotic exoskeleton using biological signals," *IEEE Trans. Ind. Electron.*, vol. 64, no. 2, pp. 1664–1674, Feb. 2017.

[49] C. Zeng, C. Yang, H. Cheng, Y. Li, and S.-L. Dai, "Simultaneously encoding movement and sEMG-based stiffness for robotic skill learning," *IEEE Trans. Ind. Informat.*, vol. 17, no. 2, pp. 1244–1252, Feb. 2021.

[50] A. G. Feldman, "Once more on the equilibrium-point hypothesis (λmodel) for motor control," *J. Motor Behav.*, vol. 18, no. 1, pp. 17–54, Mar. 1986.

[51] H. Yu, M. Spenko, and S. Dubowsky, "An adaptive shared control system for an intelligent mobility aid for the elderly," *Auto. Robots*, vol. 15, pp. 53–66, Jul. 2003.

Jing Luo (Member, IEEE) received the joint Ph.D. degree in robotics and control from the South China University of Technology and the Imperial College London in 2020. He acted as a Visiting Researcher with LIRMM, Montpellier, France, in 2019. He was involved in several scientific research projects and produced several research results that have been published in several journals, such as IEEE TRANSACTIONS, journals, and letters. His research interests include robotics, teleoperation, wearable devices, and human–robot interaction. He has served as the Lead-Guest Editor for several journals, such as *IEEE Systems, Man, and Cybernetics Magazine*, *Micromachines*, and *Frontiers in Neurorobotics*.

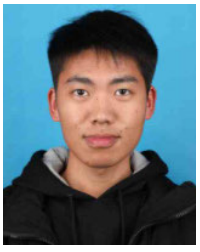

Chaoyi Zhang received the B.S. degree in measurement and control technology and instruments from Dalian Maritime University, Dalian, China, in 2022. He is currently pursuing the M.S. degree in electronic information with the School of Automation, Wuhan University of Technology, Wuhan, China. His current research interests include robotics and human–robot interaction.

Weiyong Si received the M.S. degree in aerospace engineering from Beijing Institute of Technology, China, in 2018, and the Ph.D. degree in robotics from the University of the West of England, Bristol, U.K., in 2023. He is currently a Lecturer with the Robotics and Embedded Intelligent Systems Laboratory, University of Essex, Colchester, U.K. His research interests include robot learning, robot-assisted medical examination, teleoperation, and robot control.

Yiming Jiang (Member, IEEE) received the Ph.D. degree in control science and engineering from the School of Automation, South China University of Technology, Guangzhou, China, in 2019. He was a Visiting Scholar with the University of Portsmouth, Portsmouth, U.K., from 2017 to 2018. He is currently an Associate Professor with the School of Robotics, Hunan University, Changsha, China. His research interests include multiple robots cooperative control, intelligent control, and human–robot interaction.

Chenguang Yang (Fellow, IEEE) received the B.Eng. degree in measurement and control from Northwestern Polytechnical University, Xian, China, in 2005, and the Ph.D. degree in control engineering from the National University of Singapore, Singapore, in 2010. He performed postdoctoral studies in human robotics at the Imperial College London, London, U.K., from 2009 to 2010. He is a Chair in Robotics with Department of Computer Science, University of Liverpool, U.K. His research interest lies in human robot interaction and intelligent system design. He was awarded UK EPSRC UKRI Innovation Fellowship and individual EU Marie Curie International Incoming Fellowship. As the lead author, he won the IEEE TRANSACTIONS ON ROBOTICS Best Paper Award (2012) and IEEE TRANSACTIONS ON NEURAL NETWORKS AND LEARNING SYSTEMS Outstanding Paper Award (2022). He is the Corresponding Co-Chair of IEEE Technical Committee on Collaborative Automation for Flexible Manufacturing.

Chao Zeng (Member, IEEE) received the Ph.D. degree in pattern recognition and intelligent systems from the South China University of Technology (SCUT) in December 2019. He worked as a post-doctoral research fellow in UHH from 2020 to 2023. He is now working as a research fellow at University of Liverpool. His research interests include developing learning and control approaches for robot-compliant and dexterous manipulation in physical interaction task scenarios. He has served as the Lead- or Co-Guest Editor for several journals, such as *Frontiers in Robotics and AI*, *Robotics and Autonomous Systems*, *Micromachines*. He also serves as an independent reviewer for numerous journals and conferences.